

LETTER TO THE EDITOR

Free-bound emission from cosmological hydrogen recombination

J. Chluba¹ and R. A. Sunyaev^{1,2}

¹ Max-Planck-Institut für Astrophysik, Karl-Schwarzschild-Str. 1, 85741 Garching bei München, Germany
e-mail: jchluba@mpa-garching.mpg.de

² Space Research Institute, Russian Academy of Sciences, Profsoyuznaya 84/32, 117997 Moscow, Russia

Received 4 August 2006 / Accepted 7 September 2006

ABSTRACT

In this letter we compute the emission coming from the direct recombination of free electrons to a given shell ($n \geq 2$) during the epoch of cosmological hydrogen recombination. This contribution leads to a total of *one* photon per recombined hydrogen atom and therefore a ~ 30 – 88% increase in the recombination spectrum within the frequency range $1 \text{ GHz} \leq \nu \leq 100 \text{ GHz}$. In particular, the Balmer-continuum emission increases the distortion at $\nu \sim 690 \text{ GHz}$ by roughly 92% . With our 100 shell calculations for the hydrogen atom, we find that a total of ~ 5 photons per hydrogen atom are emitted when including all the bound-bound transitions, the $2s$ two-photon decay channel, and the optically thin free-bound transitions. Since the direct recombination continuum at high n is very broad, only a few n -series continua are distinguishable and most of this additional emission below $\nu \lesssim 30 \text{ GHz}$ is completely featureless.

Key words. cosmic microwave background

1. Introduction

With the advent of accurate observations of the cosmic microwave background (CMB) temperature and polarization anisotropies, it becomes increasingly important to understand the dynamics of cosmological recombination with percent-level precision. Several authors (Leung et al. 2004; Dubrovich & Grachev 2005; Chluba & Sunyaev 2006; Kholupenko & Ivanchik 2006) have discussed physical processes leading to percent-level corrections to the results of the standard computation (Seager et al. 2000) for the ionization history. Recently, it has been shown that the treatment of the populations in the angular momentum sub-states of hydrogen also has a percent-level impact on the ionization history, especially at redshifts $z \lesssim 800$ – 1000 (Rubiño-Martin et al. 2006; Chluba et al. 2006, hereafter RMCS06 and CRMS06, respectively), and it is expected that more physical processes altering the dynamics of cosmological recombination may be realized. Lewis et al. (2006) took some first steps towards quantifying the possible impact of percent-level corrections to the ionization history of the estimation of cosmological parameters.

In the future it may become possible to directly observe the spectral distortions of the CMB arising during the epoch of recombination. This should open an alternative way of determining cosmological parameters like the baryon and total matter density. Several authors discussed the distortions arising from the hydrogen higher-level bound-bound transitions (Dubrovich 1975; Liubarskii & Sunyaev 1983; Rybicki & dell'Antonio 1993; Dubrovich & Stolyarov 1995; Burgin 2003; Dubrovich & Shakhvorostova 2004; Kholupenko et al. 2005; Wong et al. 2006; Rubiño-Martin et al. 2006; Chluba et al. 2006).

In the standard computations within the cosmological context, the *direct recombination* to the ground state of hydrogen is neglected, since this transition is so optically thick during the whole epoch of recombination that the escape of photons in

the Lyman-continuum is considered impossible (Zeldovich et al. 1968; Peebles 1968). On the other hand, electrons can reach *any* of the other levels (with $n \geq 2$) by *direct recombination* and the emitted continuum photons escape freely, just because after their creation they will not encounter another optically thick transition within the hydrogen atom.

Every successful recombination (i.e. when the electron reaches the ground-state and remains there) will therefore lead to the emission of *at least* two photons, one from the direct recombination and (because direct recombinations to the ground-state are neglected) *at least* one within the cascade to the ground-state. Here we show that for hydrogen a total of ~ 4 photons per neutral hydrogen atom is produced within the bound-bound cascade and the $2s$ two-photon decay channel. Therefore, one expects a $\sim 25\%$ addition to the total number of emitted photons during the epoch of recombination due to the *direct recombination* to states with $n \geq 2$.

In this paper we discuss the hydrogen recombination spectrum in the frequency range $100 \text{ MHz} \leq \nu \leq 3000 \text{ GHz}$, with special emphasis on the contribution from the direct recombination lines (for more details on the bound-bound emission within this context see RMCS06 and CRMS06). We use the solution for the recombination history and evolution of the hydrogen populations as obtained in CRMS06. In those computations a maximum of 100 shells was treated following the populations of *all* the angular momentum sub-states separately and including l - and n -changing collisions. We refer the reader to this paper for more details on the computations.

2. Spectral distortion due to direct recombination

In order to compute the spectral distortion from direct recombinations to a given level (n, l), one has to consider the emission and absorption of photons by this process. The effective rate for

the change in the population, N_i , of a hydrogen level i due to recombinations from the continuum is given by

$$\left. \frac{\partial N_i}{\partial t} \right|_i^{\text{rec}} = N_e N_p R_{ci} - N_i R_{ic}, \quad (1)$$

where N_e and N_p are the free electron and proton number densities, R_{ci} is the corresponding recombination rate, and R_{ic} the photoionization rate. Using the definition of R_{ci} and R_{ic} in terms of the photoionization cross section, $\sigma_{ic}(\nu)$, one can write the effective change in $N_i = I_\nu/h\nu$, where I_ν is the photon intensity, due to direct recombination to level i at frequency ν as

$$\frac{1}{c} \left. \frac{\partial N_i}{\partial t} \right|_i^{\text{rec}} = N_e N_p f_i(T_e) \sigma_{ic} \left[\frac{2\nu^2}{c^2} + N_i \right] e^{-\frac{h\nu}{kT_e}} - N_i \sigma_{ic} N_\nu. \quad (2)$$

Here stimulated recombination is included. From the Saha-relation one has $f_i(T_e) = \left(\frac{N_i}{N_e N_p} \right)^{\text{LTE}} = \frac{g_i}{2} \left(\frac{h^2}{2\pi m_e k T_e} \right)^{3/2} e^{E_i/kT_e}$, where E_i is the ionization energy; T_e the electron temperature, which is always very close to the radiation temperature $T_\gamma = T_0(1+z)$ with $T_0 = 2.725$ K; and $g_i = 2(2l+1)$ is the statistical weight of the level. It is clear from Eqs. (1) and (2) that the total change in the number of photons has to be identical to the number of recombined electrons.

Now, given the solution for the recombination history and evolution of the populations N_i , one can obtain the solution for the change in the radiation field in the optically thin limit by assuming a *pure blackbody ambient photon field*. For the spectral distortion of the CMB at observing frequency ν due to direct recombination to level i at redshift $z = 0$ we find

$$\Delta I_i^{\text{rec}}(\nu) = B_\nu \int_{z_1}^{\infty} \frac{c N_i \sigma_{ic}(\nu_z)}{H(z)(1+z)} \left[\frac{N_e N_p}{N_i} f_i(T_e) e^{\frac{h\nu_z}{kT_\gamma} - \frac{h\nu_z}{kT_e}} - 1 \right] dz, \quad (3)$$

with $\nu_z = \nu(1+z)$ and where $H(z)$ is the Hubble-expansion factor, $1+z_1 = \nu_{ic}/\nu$ corresponds to the redshift at which the emission and photoionization threshold frequency, ν_{ic} , are equal and B_ν is the CMB blackbody spectrum today.

In the limit of $n \gg 1$, the ionization threshold corresponds to $h\nu_n = \chi/n^2$ and the energy of the n_α transition is $h\nu_{n_\alpha} = 2\chi/n^3$, i.e. $n/2$ times smaller. Therefore in our computations with $n_{\text{max}} = 100$ at $z = 0$, the lowest frequency we reach is expected to be approximately $\nu_{\text{low,fb}} \sim 200\text{--}300$ MHz instead of $\nu_{\text{low,bb}} \sim 4\text{--}6$ MHz for the bound-bound transitions. The width of the recombinational line is similar to $h\Delta\nu_n \sim kT_{e,n}^{\text{peak}}$, where $T_{e,n}^{\text{peak}} \sim T_\gamma(z_n^{\text{peak}})$ is the temperature of the electrons at the redshift, where the main contribution to the *direct recombination emission* for shell n appeared (typically $z_n^{\text{peak}} \sim 1300$). Hence, one expects that the contributions to the free-bound continuum will become very broad for $h\nu_n \ll kT_{e,n}^{\text{peak}}$. For the Balmer and Paschen continua, one has $h\nu_2 \sim 10 kT_{e,2}^{\text{peak}}$ and $h\nu_3 \sim 5 kT_{e,3}^{\text{peak}}$, so that the contributions due to these transitions are narrow, while for $n \gg 1$ they are very broad (see Fig. 1).

3. Results and discussion

In Fig. 1 we present the full hydrogen recombination spectrum including the emission due to bound-bound transitions, the $2s$ two-photon decay, and direct recombinations to shells with $n \geq 2$. At high frequencies the free-bound emission shows narrow features corresponding to the Balmer, Paschen, Brackett, and Pfund continua. The strongest additional emission is due to the Balmer continuum, which increases the level of the distortion at $\nu \sim 690$ GHz by roughly 92%. At low frequencies

the free-bound continua overlap very strongly and the total continuum emission becomes completely featureless, amounting to a $\gtrsim 30\%$ up to $\sim 88\%$ contribution in the frequency range $1 \text{ GHz} \leq \nu \leq 100 \text{ GHz}$, which partially fills the gaps in the bound-bound emission spectrum and slightly lowers the contrast of these features. The inlay plot in the upper panel shows the free-bound continuum emission for three well-separated, high levels. These contributions are very broad and each of them lies within a factor of ~ 10 below the total free-bound emission spectrum. The total level of the emission is only reached after summing over many shells. As the inlay plot in the lower panel illustrates, the sum of all contributions (here mainly bound-bound and free-bound) still has a significant modulation ranging from $\sim 4\text{--}35\%$ in the frequency band $1 \text{ GHz} \leq \nu \leq 30 \text{ GHz}$. The slope of the free-bound distortion for $1 \text{ GHz} \lesssim \nu \lesssim 10 \text{ GHz}$ is ~ 0.6 , therefore slightly steeper than for the contribution from the bound-bound transitions alone (~ 0.46). At $\nu \lesssim 1 \text{ GHz}$ one still expects an increase in emission when including more than 100 shells.

In Fig. 1 we also show the free-bound contribution for different values of $n_{\text{max}} < 100$. From this one can conclude that, within our assumptions, the free-bound emission spectrum converges to a level of better than 1% at $\nu \gtrsim 5\text{--}10 \text{ GHz}$ and better than 10% for $1 \text{ GHz} \lesssim \nu \lesssim 2 \text{ GHz}$. We also checked how much the free-bound emission depends on the treatment of the angular-momentum sub-states and found that at high frequencies the solution is not very different, when assuming full statistical equilibrium within the shells for $n > 2$. At low frequencies, like in the case for bound-bound transitions (see CRMS06), the difference is much larger, again showing that it is important to follow the populations of all the angular momentum sub-states separately.

Figure 2 shows the total number of photons per hydrogen atom emitted during recombination for a given n -series (sum of all bound-bound transitions to one shell with fixed n) and its continuum (the corresponding bound-free contribution). In the considered case, one can see that the total emission is dominated by the contribution from direct recombinations for $n \gtrsim n_{\text{cr}} \sim 30$. For $n \lesssim n_{\text{cr}}$ the contribution from bound-bound-transitions dominates. This behavior shows that cascading electrons are very important for the lower shells, whereas for larger n the electrons reach a given shell mainly via direct recombinations. Obviously including more than 100 shells will lead to an increase in n_{cr} , but one does not expect a significant addition to the total number of emitted photons. There is a strong difference in both curves when the computation is done assuming full statistical equilibrium for shells with $n > 2$. In this case the curves intersect at $n_{\text{cr}} \sim 59$ instead of $n_{\text{cr}} \sim 30$. This shows that, following all the angular momentum sub-states, the lack of strong redistribution to states with $l \gg 1$ does not favor the cascade with $\Delta n \ll n$ -transitions.

Knowing the asymptotic behavior of the distortion at low frequencies, $\Delta I_\nu = A_0 [\nu/1 \text{ GHz}]^\beta 10^{-28} \text{ J m}^{-2} \text{ s}^{-1} \text{ Hz}^{-1} \text{ sr}^{-1}$, from Fig. 1, one can find the number of photons emitted per hydrogen atom (present density $N_{\text{H}} = 1.9 \times 10^{-7} \text{ cm}^{-3}$) at $\nu \leq \nu_0$, i.e. $N_\nu/N_{\text{H}} = \frac{4\pi}{c N_{\text{H}}} \int_0^{\nu_0} \frac{A_\nu}{h\nu} d\nu = 3.3 \times 10^{-2} \frac{A_0}{\beta} [\nu_0/1 \text{ GHz}]^\beta$. Within the range $1 \text{ GHz} \lesssim \nu \lesssim 10 \text{ GHz}$ we obtained $A_0^{\text{bb}} \sim 2.2$ and $\beta_{\text{bb}} \sim 0.46$ for the bound-bound and $A_0^{\text{fb}} \sim 0.59$ and $\beta_{\text{fb}} \sim 0.6$ for the free-bound distortion. Considering the bound-bound distortion and assuming that the α -transitions give the main contribution and that most of the photons are released at $z_{\text{em}} \sim 1300$, with $h\nu_{n_\alpha}^{\text{obs}} = 2\chi/z_{\text{em}} n^3$, one finds $N_\nu^{\text{bb}}(n > n_0)/N_{\text{H}} = 3.3 \times 10^{-2} [6.6 \times 10^6/z_{\text{em}}]^\beta \frac{A_0}{\beta} n_0^{-3\beta} \sim 8.0 n_0^{-1.38}$ and

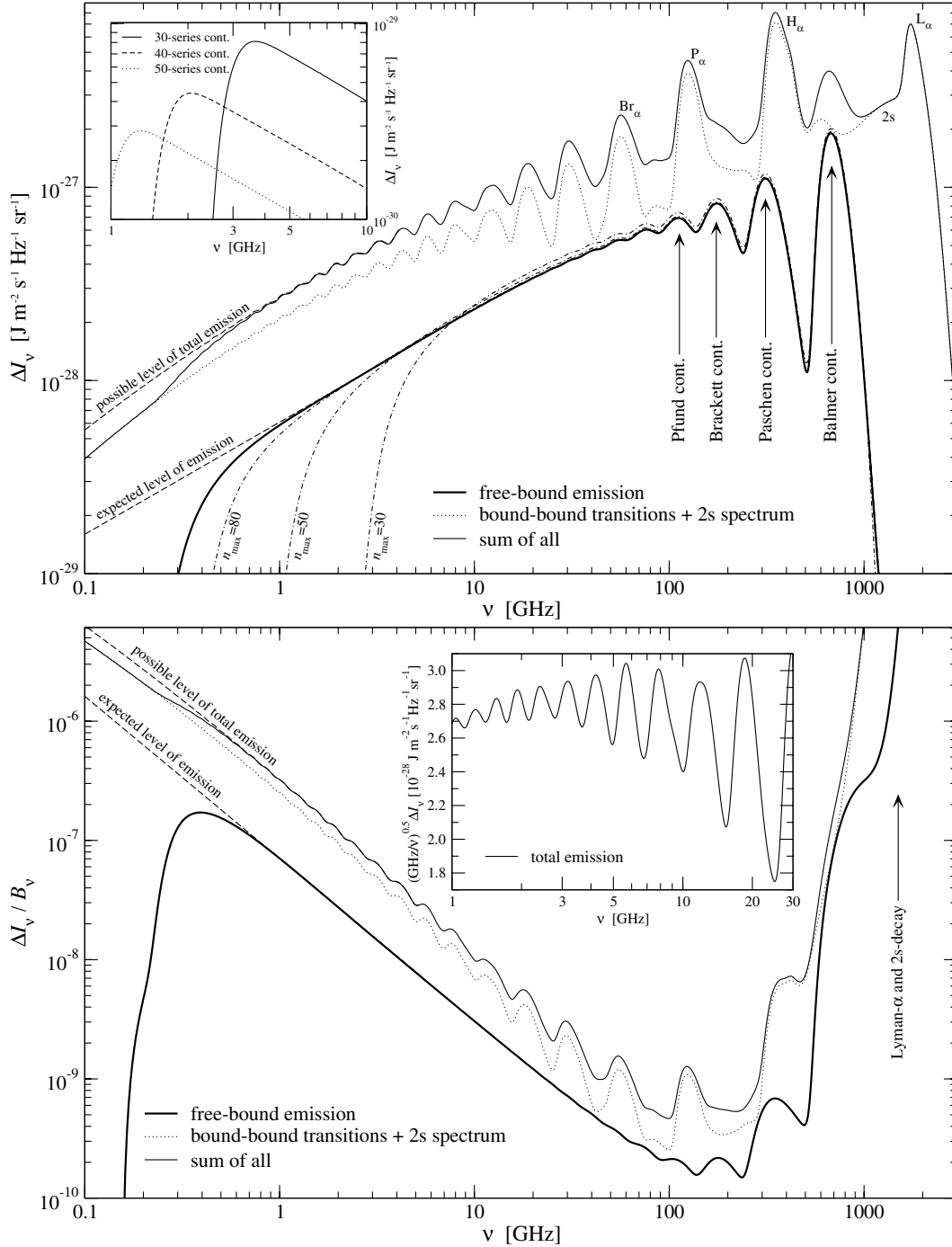


Fig. 1. The full hydrogen recombination spectrum including the free-bound emission. The results of the computation for 100 shells were used as presented in CRMS06. The contribution due to the 2s two-photon decay is also accounted for. The dashed lines indicate the expected level of emission when including more shells. In the upper panel we also show the free-bound continuum spectrum for different values of n_{\max} (dashed-dotted). The inlay gives the free-bound emission for $n = 30, 40$, and 50 . The lower panel shows the distortion relative to the CMB blackbody spectrum, and the inlay illustrates the modulation of the total emission spectrum for $1 \text{ GHz} \leq \nu \leq 30 \text{ GHz}$ in convenient coordinates.

$|dN_{\gamma}^{\text{bb}}/dn_0| \sim 11 n_0^{-2.38} N_{\text{H}}$ for the contribution of the whole series for given shell n_0 . Similarly, one has $N_{\gamma}^{\text{fb}}(n > n_0)/N_{\text{H}} \sim 3.6 n_0^{-1.2}$ and $|dN_{\gamma}^{\text{fb}}/dn_0| \sim 4.3 n_0^{-2.2} N_{\text{H}}$ for the free-bound emission with $h\nu_n^{\text{obs}} = \chi/z_{\text{em}} n^2$, although for $n_0 \gg 1$ one expects this estimate to be rather crude due to the large width of the free-bound contributions. We found that $|dN_{\gamma}^{\text{fb}}/dn_0| \sim 2.5 n_0^{-1.9} N_{\text{H}}$ represents the result shown in Fig. 2 for large n_0 very well. One should mention that induced recombinations and stimulated transitions play an important role for $n \gg 1$ and $|\Delta n| \ll n$.

In Table 1 we give the values of the total number of photons per hydrogen atom emitted in the Balmer, Paschen, Brackett, and Pfund-series and their continua. Also we list the total number of emitted photons in all n -series and their continua, along with the contribution from the 2s two-photon decay. As expected, the total number of emitted photons due to free-bound transitions (within the accuracy of our calculation) is identical to the total number of hydrogen atoms. The number of photons emitted within the Balmer-series and Balmer-continuum is also

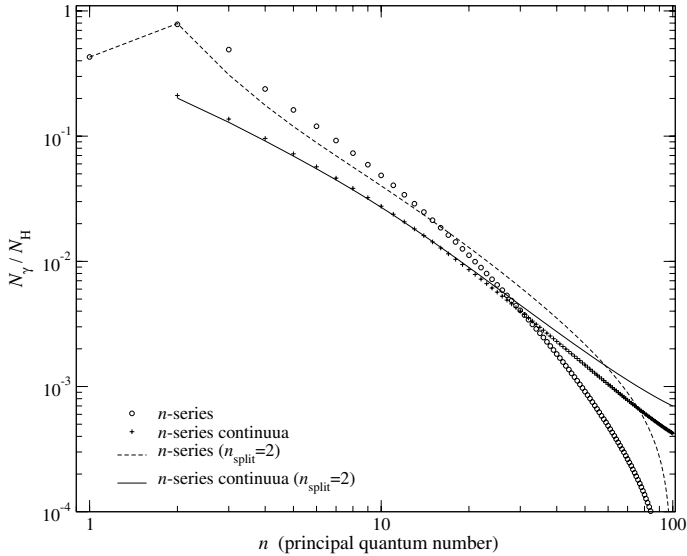


Fig. 2. Total number of photons per hydrogen atom released during recombination for a given n -series and its continuum for $n_{\max} = 100$. Also the results are presented after assuming full statistical equilibrium within the shells for $n > 2$ ($n_{\text{split}} = 2$).

very close to one photon per hydrogen atom. One can see that roughly 2.8 photons per hydrogen atom are released within the bound-bound transitions. For the free-bound distortion, 80% of the photons are emitted for $n \lesssim 14$ –15, 90% for $n \lesssim 26$, and 95% for $n \lesssim 41$. On the other hand, within the bound-bound transitions one finds 80% for $n \lesssim 6$ –7, 90% for $n \lesssim 11$ –12, and 95% for $n \lesssim 18$. Focusing on the Lyman-series and the 2s two-photon decay contribution, one can see that $\sim 43\%$ of all electrons go through the Lyman- α and $\sim 57\%$ of the electrons reach the ground state via the 2s two-photon decay channel. *During the epoch of hydrogen recombination, a total of ~ 5 photons per hydrogen atom are produced.* Therefore, recombination of hydrogen slightly increases the specific entropy of the Universe (photons per baryon).

Observations of the recombination features at frequencies $\nu \gtrsim 1412$ MHz might become feasible since the strength of the signal under discussion is close to $2 \times 10^{-7} B_\nu$ and still has

Table 1. Total number of photons per hydrogen atom emitted during recombination within a given series and its continuum. Adding all the contributions, one obtains 4.98 photons per hydrogen atom.

Series	n	bound-bound	continuum	sum
Lyman	1	4.28×10^{-1}	0	4.28×10^{-1}
Balmer	2	7.83×10^{-1}	2.11×10^{-1}	9.94×10^{-1}
Paschen	3	4.91×10^{-1}	1.37×10^{-1}	6.28×10^{-1}
Brackett	4	2.38×10^{-1}	9.59×10^{-2}	3.34×10^{-1}
Pfund	5	1.62×10^{-1}	7.22×10^{-2}	2.34×10^{-1}
All	1–100	2.84	1.00	3.84
2s-decay	1	0	1.14	1.14

variability with well-defined frequency dependence at a level of several percent (Fig. 1). Also in this band ($\lambda < 21$ cm), one does not expect other sources with similar frequency dependence.

Acknowledgements. We wish to thank J.A. Rubiño-Martín for useful discussion of this problem at the initial stage.

References

- Burgin, M. S. 2003, *Astron. Rep.*, 47, 709
 Chluba, J., Rubiño-Martín, J. A., & Sunyaev, R. A. 2006, *MNRAS*, submitted [arXiv:astro-ph/0608242], CRMS06
 Chluba, J., & Sunyaev, R. A. 2006, *A&A*, 446, 39
 Dubrovich, V. K. 1975, *Soviet Astron. Lett.*, 1, 196
 Dubrovich, V. K., & Grachev, S. I. 2005, *Astron. Lett.*, 31, 359
 Dubrovich, V. K., & Shakhvorostova, N. N. 2004, *Astron. Lett.*, 30, 509
 Dubrovich, V. K., & Stolyarov, V. A. 1995, *A&A*, 302, 635
 Kholupenko, E. E., & Ivanchik, A. V. 2006, *Astron. Lett.*, submitted
 Kholupenko, E. E., Ivanchik, A. V., & Varshalovich, D. A. 2005, *Gravitation and Cosmology*, 11, 161
 Leung, P. K., Chan, C. W., & Chu, M.-C. 2004, *MNRAS*, 349, 632
 Lewis, A., Weller, J., & Battye, R. 2006 [arXiv:astro-ph/0606552]
 Liubarskii, I. E., & Sunyaev, R. A. 1983, *A&A*, 123, 171
 Peebles, P. J. E. 1968, *ApJ*, 153, 1
 Rubiño-Martín, J. A., Chluba, J., & Sunyaev, R. A. 2006, *MNRAS*, submitted [arXiv:astro-ph/0607373], RMCS06
 Rybicki, G. B., & dell’Antonio, I. P. 1993, in *Observational Cosmology*, ed. G. L. Chincarini, A. Iovino, T. Maccacaro, & D. Maccagni, ASP Conf. Ser., 51, 548
 Seager, S., Sasselov, D. D., & Scott, D. 2000, *ApJS*, 128, 407
 Wong, W. Y., Seager, S., & Scott, D. 2006, *MNRAS*, 367, 1666
 Zeldovich, Y. B., Kurt, V. G., & Syunyaev, R. A. 1968, *Zhurnal Eksperimentalnoi i Teoreticheskoi Fiziki*, 55, 278